Materials Physics and Mechanics 36 (2018) 8-17 Received: July 16, 2017

THE EFFECT OF LITHIUM PERCHLORATE ON POLY (SODIUM 4-STYRENESULFONATE): STUDIES BASED ON MORPHOLOGY, STRUCTURAL AND ELECTRICAL CONDUCTIVITY

M.F. Hassan* and N. Noruddin

Advanced Nano Materials (ANoMa) Research Group, School of Fundamental Science, Universiti Malaysia Terengganu, 21030 Kuala Nerus, Terengganu, Malaysia

*e-mail: mfhassan@umt.edu.my

Abstract. Solid polymer electrolytes (SPEs) of Poly(sodium 4-styrenesulfonate) (PSS) as a polymer host and lithium perchlorate (LC) as an ionic dopant were prepared using a single-solvent via solution casting technique. According to XRD analyses, the solid polymer electrolyte films were in amorphous phase and the coexistence of peaks of the materials (PSS and LC) confirmed that the complex films were successfully obtained. The SEM observations revealed that the films appeared to be rough, flat, and irregular shape of surfaces. The highest ionic conductivity (σ) of 7.21×10^{-6} S cm^{-1} was achieved at room temperature (303K) for the sample containing 15 wt.% LC.

Keywords: solid polymer electrolyte; poly(sodium 4-styrenesulfonate); lithium perchlorate; ionic conductivity; impedance spectroscopy.

1. Introduction

Solid state ionic conductors are crucial topic in various energy storage fields such as in battery, fuel cell and sensor technologies [1]. In battery application for instance, solid state conductors are mainly present as a solid electrolyte. This electrolyte has two main functions which are as a separator and as a medium for ionic species movement via its structure or surface. In general, a polymer like Poly(Sodium 4-Styrenesulfonate) (PSS) is used as a host/medium to prepare such electrolyte and it is doped with ionic salts (for example lithium perchlorate (LC)) to enhance the ionic conductivity of the polymer until it reaches the highest value. This solid polymer electrolyte (SPE) can normally be obtained whether in crystalline or amorphous and/or in both phases. Wright [2] initiated the first document to prepare solid polymer electrolytes for all-solid state battery applications. Generally, a SPE without an ionic dopant is known to have unsatisfactory performance at ambient temperature which is one of its weaknesses compared to the existing conventional liquid/hybrid electrolytes [3]. To this extent, numerous studies on SPE doped with ionic salts have been conducted and the experiments had excellent results. A number of these successfully works had proven that the high ionic conductivity can be easily obtained, and the flexibility of SPE can be preserved by controlling the salt content inside the polymer [4-10].

In SPE preparation, PSS is used as a host polymer and LC as an ionic dopant. PSS is well acknowledged as an anionic polyelectrolyte [11]. It can be produced by the polymerization of an anionic surfactant, sodium styrene sulfonate. There is a group of polar solvents as listed in Zoghlami et. al 2017 that can be used to dissolve this polyelectrolyte [11]. The advantages of PSS as an agent of dispersion of graphene in water for sensor

http://dx.doi.org/10.18720/MPM.3612018_2

application [12], as a filler for coating thin mercury film electrode and as a detector to trace metal in water [13-15] have attracts many researchers to discover its current and future potential in other new possible applications. PSS also can act as an effective binder for graphene sheets and is able to increase the specific capacitance and the rate capability of capacitance [16]. In a few research works, PSS was used as a host polymer and proven that its bare ionic conductivity could be boosted if doped with the appropriate ionic salts [17-20].

$LiClO_4$ (LC) exits as a white crystalline solid and is colorless at room temperature. It is highly soluble in many solvents such as methanol, ethanol, diethyl ether, pyridine, acetonitrile and the rest as reported by Markowitz et. al, 1961 [21]. It is useful in fuel cell, supercapacitors and battery as an electrolyte component [22,23]. Previous studies provided experimental evidenced that the polymers-based complexes with LC possess an outstanding ionic conductivity, making them attractive for further investigation [23-25].

In this work, we attempt to study the effect of LC on the morphology, structural and electrical conductivity of PSS complex films. The structural modifications of SPE were investigated through a technique of X-ray diffraction. To examine the morphology evolution of the surface of doped-SPE, the SEM technique was used at high and low magnification configurations. Their conductivity behavior was determined using electrochemical impedance spectroscopy.

2. Materials and experimental methods

PSS and LC with 99.99% purities were used to produce complexation membranes via a solution casting technique. In brief, the solutions were prepared by liquidating 1g of PSS powder into 100 ml of distilled water. Then, different amounts of LC (varied from 0 to 25 (in weight percentage, wt.%)) were added to the solutions as scheduled in Table 1. The blends were stirred constantly with a magnetic stirrer until homogenous solutions were achieved. After that, the solutions were transferred into different plastic Petri dishes and were left for evaporation in order to form solid state films. Subsequently, the films were reserved in desiccators (with silica gel) for a certain period to diminish the water content. A schematic diagram of overall preparation process is described in Fig. 1. To note here, all the experimental works were carried out at room temperature.

Table 1. The compositions of PSS and LC powders.

Designation	Solvent (ml)	Polymer (g)	Ionic salt (wt.%)	Ionic salt (g)
Pure	100	1	0	0
A	100	1	5	0.053
B	100	1	10	0.111
C	100	1	15	0.177
D	100	1	20	0.250
E	100	1	25	0.333

An X-ray diffraction technique was used to determine the crystallinity of samples. A MiniFlex II diffractometer equipped with an X'celerator, using CuK_α radiation was ran to record XRD patterns in range of $2\theta = 10^o$ to 80^o. In investigation of crystallinity and/or amorphous phases of complex samples, the XRD patterns underwent a fitting process using *Origin* software. In general, these phases were evaluated by dividing area under the all peaks with area under the whole diffractogram. The percentages of phases of studied samples were calculated using equation (1) [4,26,27]:

$$\%\ of\ \ phase\ A = 100\frac{A_{phaseA}}{A_{phaseA} + A_{phaseB}}, \quad (1)$$

where, $A_{phase\ A}$ is the area of phase A and $A_{phase\ B}$ is the area of phase B.

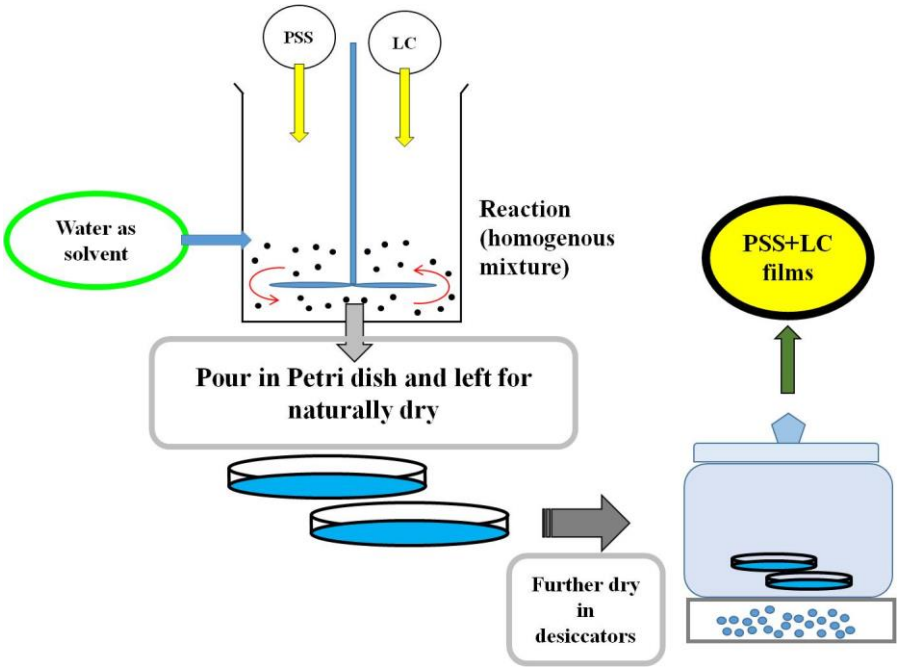

Fig. 1. A schematic diagram of the preparation of PSS-LC complexes films.

In order to investigate the effect of LC on PSS surface morphology, a scanning electron microscopy was employed to observe the surface images of the sample. It was carried out using the Model JEOL JSM-6360LA device with an acceleration voltage of 20kV. The images were taken for selected magnifications of x300, x5000 and x10000, accordingly. Through this technique, the crystalline or amorphous nature of the sample can be directly observed.

Impedance spectroscopes for room temperature (30^{o}C) were measured using a HIOKI 3532-02 LCR Hi-Tester which was interfaced to a computer. It was used to determine the electrical properties over a wide range of frequencies from 50Hz to 1MHz. The prepared samples were cut into 2 cm diameter size and placed between two stainless steel electrodes on a sample holder which was connected via leads to a computer. The bulk resistance, R_b, can be directly obtained from the imaginary impedance (Z_i) versus the real impedance (Z_r) plots from the impedance system. A micrometer-screw gauge was used to measure the sample's thickness which was then employed to calculate conductivity of sample using the equation (2):

$$\sigma = \frac{t}{R_b A}, \quad (2)$$

where t = thickness of the thin film (in cm) and A = area of the contact and R_b= bulk resistance.

3. Results and discussion

The XRD patterns recorded from 2θ = 10^{o} to 80^{o} on PSS film, LC powder and PSS-LC complex solid films are depicted in Fig. 2. The PSS film diffraction pattern can be identified with the two broad peaks at different location of 2θ, the first in between 15° to 25°, and the other in between 25° to 33°, these peaks correspond to the amorphous nature of polymer

which was calculated to be roughly 74.1% of the pattern. A few peaks located at 21.3, 23.1, 24.9, 31.6, 33.2, 35.7, 39.5, 47.2, 49.1, 52.3, 57.8, 63.0 and 73.7° are clearly visible in the LC diffraction pattern, demonstrating that it is riches with crystalline moieties. Phase calculation using the equation (1) reveals that the pattern tends to be more crystalline (62.4%) compared to amorphous (37.6%). The present study on PSS and LC diffraction patterns is in good agreement with other studies on similar materials as reported in literature [28-32]. The rest of XRD patterns refer to PSS-LC complex films. As seen in all patterns, by adding LC in the films, no significant change can be observed and the films have a certain similarity and presence in highly amorphous phase. Specifically, with 5wt.% LC, the pattern of complex films remains similar to the pure PSS film, but the amorphous phase had increased to 78%. With addition 10wt.% of LC, the pattern changed a little bit with sharp peaks appearing at 23° and 32°, respectively. These peaks correspond to LC compared to its XRD pattern and those published in literature. The amorphous phase of the sample had also increased to 83.2% at 10 wt.% of LC. Further addition of 15wt.% of LC changed the XRD pattern and the amorphous phase of film slightly decreased to 80.3%. In other words, the film became more crystallized. With the addition of LC content from 20 to 25wt.%, the resulting patterns were observed to match the patterns of the sample with 15wt.% LC. However, the amorphousity of film decreased to 77.4 and 56.2%, respectively. The overall XRD results revealed that the complex films tend to present in amorphous phase rather than crystalline phase, and the existence of LC does not leverage much on the patterns due to highly amorphous nature of polymer and its partially crystallinity. The co-availability of XRD peaks for the studied materials ratify their complexation in solid polymer electrolyte film [33-36].

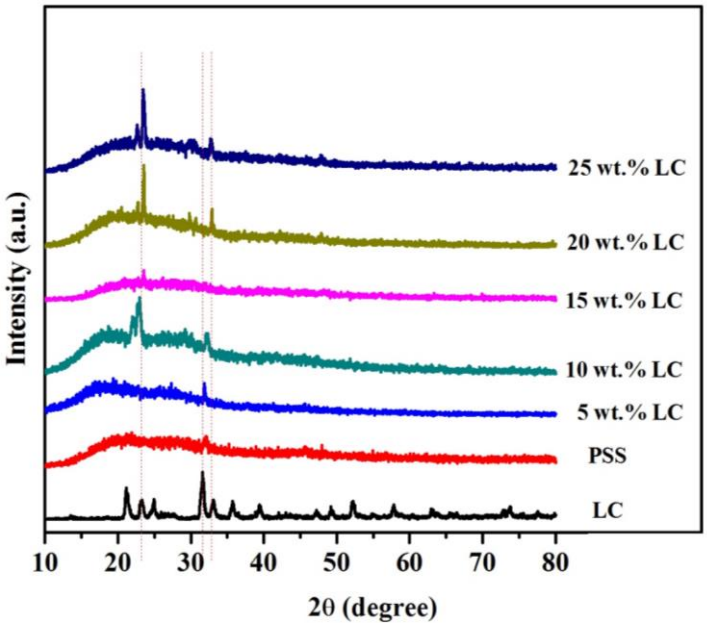

Fig. 2. XRD pattern for LC, PSS and hybrid PSS-LC films.

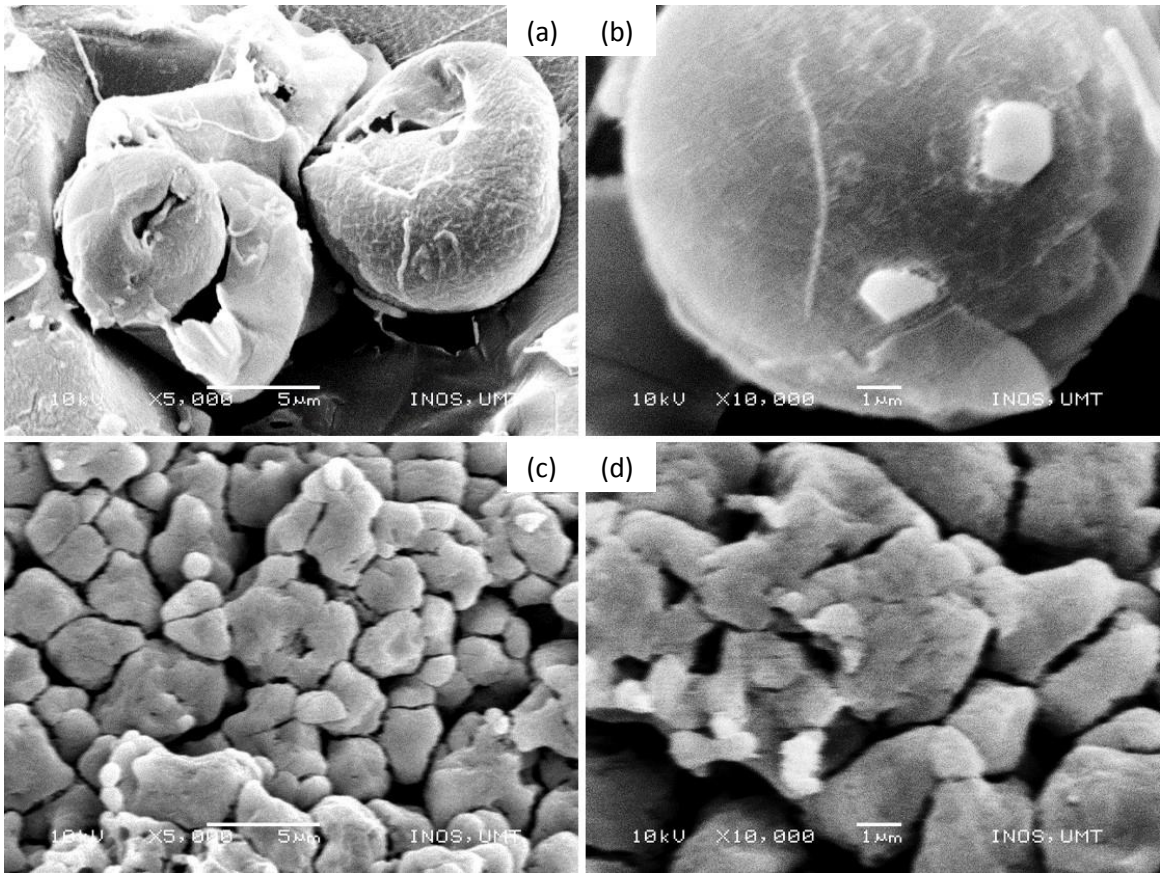

Fig. 3. SEM images PSS (a, b) and LC (c, d).

Figure 3 shows the scanning electron micrograph images of PSS and LC powders. In bare powder form, the PSS has a rounded curve shape with diameters of 5 and 10 μm, respectively (Fig. 3a and 3b)**,** while the morphology of LC can be explained as flat and compact grains 1~5μm in diameter. In film form, at low magnification (x300), the PSS had shredded and peeling-off flakes at certain surface area (Fig. 4a) but in high magnification, the surface was observed to have irregular grains with very fine particles (less than 1 μm) **(**Fig. 4b**)** covering the whole area of image. This surface morphology has been modified with presence of wrinkles, and the peel-off film was diminished in some particular areas after the adding 5wt.% of LC (Fig. 4c and 4d). With the addition of 10wt.% of LC, the wrinkles arranged in uniform orientation with the peel-off film had completely disappeared. New sphere shapes were clearly observed on the surface (Fig. 4e and 4f) due to surface modification. In Fig. 4g (15wt.% of LC), the wrinkles seem become thick joined to the sphere shapes on the top at increasing quantity. At high magnification image (x10000), the actual surface of film was seen to be covered with small particles (Fig. 4h). With further addition of 20wt.% of LC, cracked films without complete separation can be seen in specific areas (Fig. 4i and 4j). The film fracture spread further after the amount of LC was increased to 25wt.% (Fig. 4k) and it is clearly visible where the pieces of films are disconnected with each other as shown in Fig. 4l.

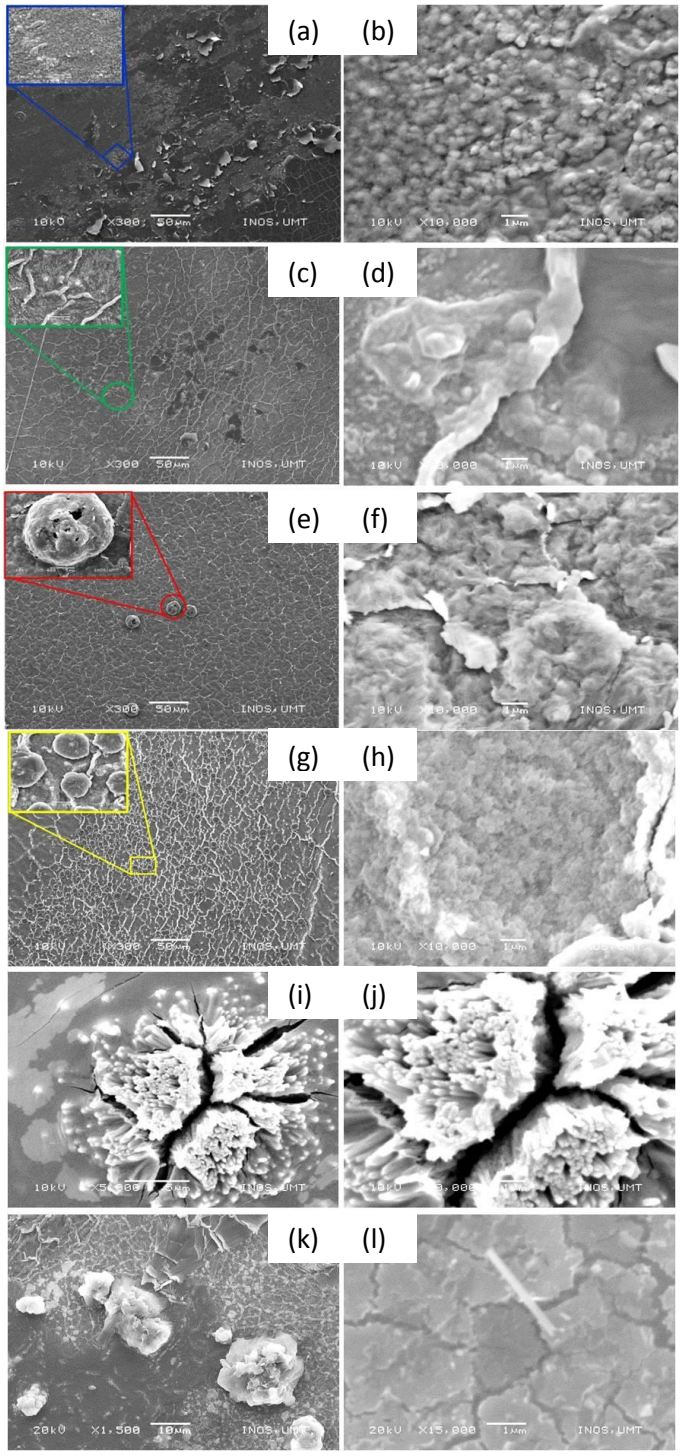

Fig. 4. SEM micrographs at different magnifications for (a,b) PSS films, (c,d) 5 wt.% LC (sample A), (e, f) 10 wt.% LC (sample B), (g, h) 15 wt.% LC (sample C), (i, j) 20 wt.% LC (sample D) and (f) 25 wt.% LC (sample E).

Table 2. The bulk resistance and ionic conductivity of PSS–LC complexes films at room temperature.

Designation	Bulk resistance, R_b (Ω)	Conductivity, σ (S cm^{-1})
Pure	1.12 x 10^{4}	7.22 x 10^{-8}
A	1.88 x 10^{3}	4.84 x 10^{-7}
B	6.91 x 10^{2}	1.41 x 10^{-6}
C	1.21 x 10^{2}	7.20 x 10^{-6}
D	2.82 x 10^{2}	2.98 x 10^{-6}
E	3.48 x 10^{2}	2.42 x 10^{-6}

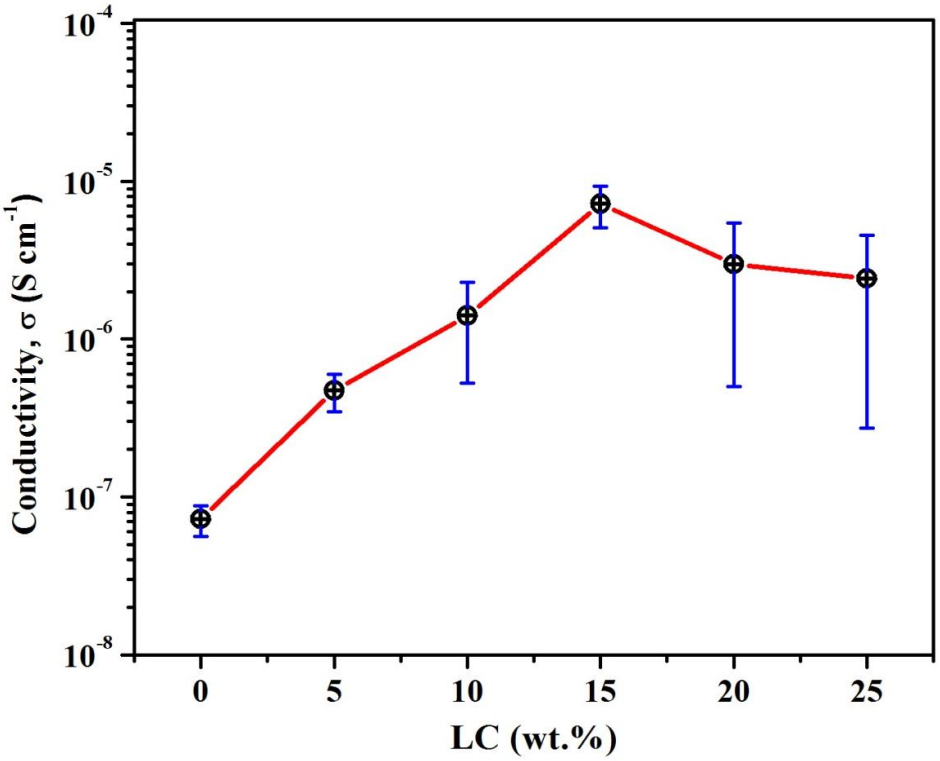

Fig. 5. The conductivity variation as a function of salt content at room temperature.

The values of bulk resistance, R_b and the ionic conductivity, σ of the samples are tabulated in Table 2 while Fig. 5 presents a trend of ionic conductivity variation as a function of salt content at room temperature. The measured thicknesses of the samples were in between 8.0 x 10^{-3} to 9.0 x 10^{-3} cm and used together with bulk resistances to calculate the ionic conductivity of sample using equation (2). The bulk resistance of the pure PSS film was 1.12 x 10^{4} Ω with an ionic conductivity of approximately 7.22 x 10^{-8} S cm^{-1}. With addition of 5 wt.% of LC, the bulk resistance decreased to 1.88 x 10^{3} Ω and the ionic conductivity increased to 4.84 x 10^{-7} S cm^{-1}. The bulk resistance (6.91 x 10^{2} Ω) was decreased after addition of 10 wt.% LC and given the ionic conductivity of 1.41 x 10^{-6} S cm^{-1}. With addition of 15 wt.% LC, the bulk resistance was reduced to 1.21 x 10^{2} Ω and given the highest ionic conductivity of 7.20 x 10^{-6} S cm^{-1}. In addition of 20 wt.% LC, the measured resistance increased to 2.82 x 10^{2} Ω and reduced the ionic conductivity to 2.98 x 10^{-6} S cm^{-1}. The declined trend of ionic conductivity continued in 25 wt.% LC film with the value was 3.16 x 10^{-4} S cm^{-1} and the bulk resistance of 3.48 x 10^{2} S cm^{-1}, respectively. With further addition of LC in polymer, the formation of complex films cannot be obtained and the

investigation on its electrical conductivity is difficult to be conducted via the available equipments. To be note, the high standard deviations for a few samples especially for 20 and 25wt% LC were due to the films disintegrated and provided the high resistance values. From Fig. 6, it can be understood that the addition of LC up to 10wt.%, the degree of amorphousity of complex samples was increased and matched to the trend of ionic conductivity. With addition of LC up to 15wt%, the degree of amorphousity was started decreased but not on its conductivity which continued increased to achieve the highest value. At 20 and 25wt% of LC, the amorphousity of sample furthers declined and this trend was comparable to the trend of ionic conductivity.

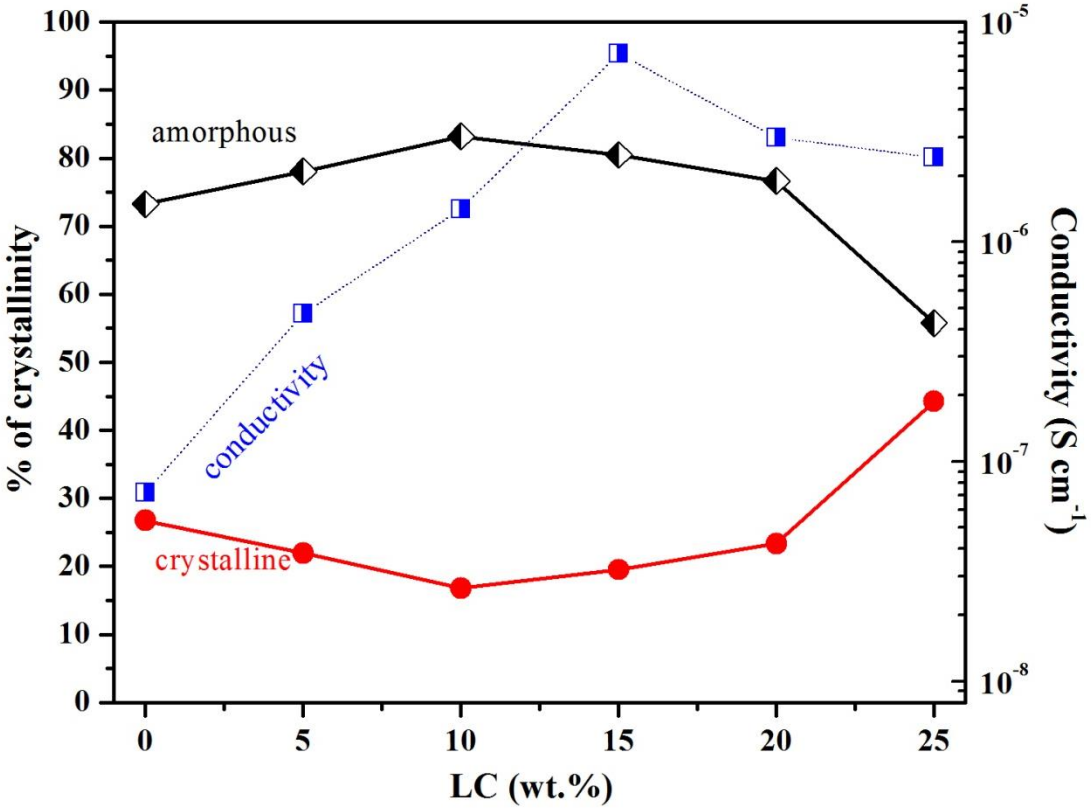

Fig. 6. The % of crystallinity and the conductivity variation as a function of salt content at room temperature.

To summarize, the increasing trend of ionic conductivity is believed to correspond to two major factors. First is the amorphous structure of complex samples which acts as a supportive medium for fast ionic movement. As reported by many researchers [24,37-39], the ionic conductivity in amorphous complex structures is higher than that in crystalline polymer salt complexes due to the relatively low interfacial resistance in between the solid electrolyte and the electrode. The second factor is related to the inorganic salt which supplies ionic conductors to the closed system until a saturated condition is achieved. This is because the increase in conductivity with salt content is attributed to the increased in the number of free mobile ions. For the decrease in ionic conductivity trend, it may be due to ion association which decreases the number of free ions available for conduction, or the decrease in mobility of the ions [40]. The drop in conductivity can also be due to the existence of wrecked films and the increase in crystallinity of film which are well supported by XRD and SEM analyses as shown in Fig. 4 and Fig. 6, respectively. These discoveries are also in good agreement with the investigation conducted by Mellander and Albinsson, and Reddy et. al [24,41].

4. Conclusions

In this study, ion-conducting polymer electrolytes based on PSS-LC were successfully prepared via a solution casting technique. The effects of LC on the PPS structure and electrical properties were investigated on using X-ray diffraction, scanning electron microscope and electrochemical impedance spectroscopy. To our knowledge, this is the first time that films based on PSS complex with LC is discussed, particularly on its structure and ionic conductivity.

In summary, it can be concluded that the complex films were highly amorphous rather than crystalline. The XRD analysis also proved that there are coexistence peaks attributed to the materials studied on, confirming the success of the complexation process occurring in this film. According to the morphology observations, the addition of LC can significantly modify the surface texture of the film, as the highest conducting sample containing 15 wt.% LC (7.20×10^{-6} S cm^{-1}) tended to have wrinkles surrounding the image mixed with a small and a large circle shape which confirm the amorphous phase of film that supports to facilitation of mobile free ions in high volume.

Acknowledgements. *The authors would like to thank the School of Fundamental Science and School of Ocean Engineering, Universiti Malaysia Terengganu for financial and facilities supports on this study.*

References

[1] Z. Gadjourova, Y.G. Andreev, D.P. Tunstall, P.G. Bruce // *Nature* **412** (2001) 520.
[2] P.V. Wright // *Brit. Polym. J.* **7** (1975) 319.
[3] K.P. Dillip, R.N.P. Choudhary, B.K. Samantaray // *Int. J. Electrochem. Sci.* **3** (2008) 597.
[4] M.F. Hassan, A.K. Arof // *Phys. Status Solidi A* **202** (2005) 2494.
[5] S. Rajendran, M. Sivakumar, R. Subadevi // *Mater. Lett.* **58** (2004) 641.
[6] N.S. Choi, J.K. Park // *Electrochim. Acta* **46** (2001) 1453.
[7] K. Pandey, M.M. Dwivedi, N. Asthana, M. Singh, S.L. Agrawal // *Mater. Sci. Appl.* **2** (2011) 721.
[8] J. Zhang, X. Huang, J. Fu, Y. Huang, W. Liu, X. Tang // *Mater. Chem. Phys.* **121** (2010) 511.
[9] W. Feng, J. Wang, Q. Wu // *Mater. Chem. Phys.* **93** (2005) 31.
[10] S. Ramesh, H.M. Ng // *Solid State Ionics* **192** (2011) 2.
[11] O. Zoghlami, M. Guettari, T. Tajouri // *Colloid Polym. Sci.* **295** (2017) 1741.
[12] J. Li, D. Miao, R. Yang, L. Qu, P.B. Harrington // *Electrochim. Acta* **125** (2014) 1.
[13] S.C. Monterroso, H.M. Carapuca, A.C. Dearte // *Electroanal.* **15** (2003) 1878.
[14] J. Jia, L. Cao, Z. Wang, T. Wang // *Electroanal.* **20** (2007) 542.
[15] L.S. Rocha, J.P. Pinheiro, H.M. Carapuca // *Langmuir* **22** (2006) 8241.
[16] F.P. Du, J.J. Wang, C.Y. Tang, C.P. Tsui, X.P. Zhou, X.L. Xie, Y.G. Liao // *Nanotechnology* **23** (2012) 475704.
[17] A.W. Imrea, M. Schönhoff, C. Cramer // *J. Chem. Phys.* **128** (2008) 134905.
[18] V. Wesp, M. Hermann, M. Schäfer, J. Hühn, W.J. Parak, K.M. Weitzel // *Phys. Chem. Chem. Phys.* **18** (2016) 4345.
[19] T. Kolling, A. Schlemmer, C. Pietzonka, B. Harbrecht, K.M. Weitzel // *J. Appl. Phys.* **107** (2010) 014105.
[20] S. Schulze, J. Zakel, M. Schäfer, K.M. Weitzel // *IEEE T. Dielect. El. In.* **19** (2012) 1167.
[21] M.M. Markowitz, W.N. Hawley, D.A. Boryta, R.F. Harris // *J. Chem. Eng. Data* **6** (1961) 325.
[22] Z. Jotanovic, G. Andric, V. Tadic, Micic // *ATI-Appl. Techno. Inno.* **3** (2010) 15.

[23] J. Rodriguez, E. Navarrete, E.A. Dalchiele, L. Sanchez, J.R.R. Barrado, F. Martin // *J. Power Sources* **237** (2013) 270.
[24] C.V.S. Reddy, G.P. Wu, C.X. Zhao, Q.Y. Zhu, W. Chen, R.R. Kalluru // *J. Non-Cryst. Solids* **353** (2007) 440.
[25] M.Y.A. Rahman, A. Ahmad, T.K. Lee, Y. Farina, H.M. Dahlan // *J. Appl. Polym. Sci.* **124** (2012) 2227.
[26] C.T. Kniess, J.C. de Lima, P.B. Prates, *The Quantification of Crystalline Phases in Materials: Applications of Rietveld Method, Sintering - Methods and Products*, ed. by Dr. Volodymyr Shatokha (InTech, 2012).
[27] P. Prevey // *J Therm Spray Techn.* **9** (2000) 369.
[28] S.B. Hendricks, E. Posnjak, F.C. Kracek // *J. Am. Chem. Soc.* **54** (1932) 2766.
[29] E.E. Ferg, D.C. Levendis, F.R.L. Schoening // *Chem. Mater.* **5** (1993) 1293.
[30] D.C. Sorescu, D.L. Thompson // *J. Phys. Chem. A* **105** (2001) 7413.
[31] H.B. Wu, M.N. Chan, C.K. Chan // *Aerosol Sci. Tech.* **41** (2007) 581.
[32] N. Golovina, G. Nechiporrenko, G. Nemtsev, I. Zyuzin, G.B. Manelis, D. Lempert // *Cent. Eur. J. Energ. Mat.* **6** (2009) 45.
[33] J.M. Joshi, V.K. Sinha // *J. Polym. Res.* **13** (2006) 387.
[34] P.C. Parvathy, A.N. Jyothi // *Starch* **64** 207.
[35] S.A. Hashimi, A. Kumar, K.K. Maurya, S. Chandra // *J. Phys. D. App. Phys.* **23** (1990) 1307.
[36] S.S. Sekhon, G. Singh, S.A. Agnithotry, S. Chandra // *Solid State Ionics* **80** (1995) 37.
[37] P.G. Bruce, C.A. Vincent // *J. Chem. Soc. Faraday Trans.* **89** (1993) 3187.
[38] N. Srivastava, A. Chandra, S. Chandra // *J. Power Sources* **81-82** (1995) 739.
[39] K.K. Maurya, S.A. Hashimi, S. Chandra, *Evidence of Ion Association in Polymer Electrolyte by Direct Mobility Measurements in Solid State Ionics: Materials and Applications*, ed. by B.V.R. Chowdari, S. Chandra, S. Singh and P.C. Srivastava (World Scientific, Singapore, 1992).
[40] S. Rajendran, R. Kannan, O. Mahendra // *Solid State Ionics* **130** (2002) 143.
[41] B.E. Mellander, I. Albinsson, *Ion Association in Alkali Triflate Salt-poly(propylene oxide) Polymer Electrolytes in Solid State Ionics: New Developments*, ed. by B.V.R. Chowdari, M.A.K.L. Dissanayake and M.A. Carrem (World Scientific, Singapore, 1996).